

Near Real-Time Wildfire Damage Assessment using Aerial Thermal Imagery and Machine Learning

Saqib Azim¹, Mai H. Nguyen¹, Daniel Crawl¹, Jessica Block¹, Rawaf Al Rawaf¹, Francesca Hart¹, Mark Campbell¹, Robert Scott², and Ilkay Altintas¹

¹*San Diego Supercomputer Center, UC San Diego*, ²*California Governor's Office of Emergency Services*
{sazim, mhnguyen, lcrawl, jlblock, ralrawaf, fhart, m6campbell, ialtintas}@ucsd.edu, robert.scott@caloes.ca.gov

Abstract—This project aims at developing an AI system to provide a reliable assessment of the structural damage caused by wildfires in the first burn period. Our approach uses multimodal data, including multispectral aerial images, historical post-fire damage assessment data, and building footprints, to create an association between damage data and structure footprints. We use these associations to generate features and use machine learning methods to assess the level of damage to structures. The resulting AI-driven system can be used to provide wildfire-induced structural damage assessments in near-real-time using only aerial images for future fires. We provide damage assessment results on several megafires in California to demonstrate the applicability of our approach to real wildfire scenarios.

Index Terms—fire, wildfire, damage, structures, assessment, machine learning

I. INTRODUCTION

Wildfires present an increasingly severe threat to communities, particularly in the Wildland Urban Interface (WUI), where residential, commercial, and industrial structures are interspersed with natural vegetation. As the frequency and intensity of wildfires grow due to climate change, the need for timely and accurate disaster response has become more critical than ever. One of the most essential components of post-wildfire response is damage assessment, which informs emergency declarations, resource allocation, and recovery efforts. However, traditional damage assessment methods relying on visible electro-optical (EO) aerial and satellite imagery or ground inspection teams are often hindered by smoke, cloud cover, and the time-intensive process of acquiring high-resolution imagery, leading to delays in crucial decision-making. To address these challenges, we propose a novel approach for near-real-time wildfire damage assessment using aerial thermal infrared (IR) imagery and machine learning algorithms. Our approach leverages data collected by the Fire Integrated Real-Time Intelligence System (FIRIS) [11] aircrafts that provide thermal infrared imagery, which we integrate with building footprints and historical EO imagery. The project aims to deliver accurate assessments of damaged and destroyed buildings within the first operational period, typically within 24 hours of the fire-front passing through a region. This capability is critical for the California Governor's Office of Emergency Services (Cal OES) [15], where rapid and reliable damage assessments are necessary to make

informed response and recovery decisions.

The development of this system has involved overcoming significant technical challenges, including handling large datasets, addressing data quality issues, and refining machine learning models to reduce overfitting and improve accuracy and robustness. Throughout the project, we have refined our methodologies for processing aerial thermal imagery, aggregating multiple mosaic images, and developing machine learning (ML) approaches tailored to the specific characteristics of wildfire damage data. Our efforts have focused on ensuring that the model can reliably distinguish between damaged and undamaged structures, even in the presence of confounding factors such as varying sensor settings, environmental conditions, and inconsistencies in ground truth data.

This paper outlines our vision for this innovative damage assessment tool, detailing the technical advancements and collaborative efforts that have been crucial to its development. We will discuss the integration of multispectral thermal imagery with machine learning workflows, the methodologies for aggregating and processing mosaic images, and the strategies employed to address data quality challenges and integration of multiple data sources to mitigate overfitting and enhancing model generalization. In addition, we will explore the potential impact of our work on wildfire response and recovery, as well as the broader implications for other disaster scenarios, including earthquakes, floods, and landslides. By co-developing this tool with Cal OES and other stakeholders, we aim to create a robust, scalable solution that can be deployed across wildfire-prone regions, providing emergency managers with the timely information they need to protect lives and property.

The paper is organized as follows: We first describe the multimodal data, including multispectral band images (e.g., midwave infrared (MWIR)), and describe the process of stitching them into mosaics to capture fire-damaged structures. The Data Preprocessing section details the association of historical postfire damage assessments with building footprints as training data. Next, we explain the extraction of infrared signatures from aerial imagery for feature generation in machine learning models to classify damage levels. The effectiveness of the

system has been validated on multiple California wildfires. Finally, we summarize the work and propose significant future directions to enhance generalizability and performance.

II. RELATED WORK

In recent years, advances in machine learning have greatly enhanced disaster response methodologies, particularly in automating damage assessments from images. A significant example of this advancement is the Vision Transformer (ViT)-based damage classifier developed by Luo et al. [1]. Their model leverages ground-level images of homes affected by California wildfires, achieving high accuracy (95%) in classifying damage severity across five categories, from “No Damage” to “Destroyed.” Unlike previous methods that primarily use CNN-based architectures, this work demonstrates the superior performance of the ViT model in capturing global dependencies across image patches, allowing for more precise differentiation between damage levels, especially in the context of wildfire damage.

While the method in [1] focuses on ground-level images, our work complements it by utilizing aerial thermal imagery, offering advantages such as the ability to cover larger areas and bypass ground-level obstacles. Additionally, our use of thermal IR imagery from FIRIS addresses visibility challenges common in wildfire environments, such as smoke or cloud cover, which are less problematic for ground-level applications. The contributions in [1] highlight the importance of high-quality, labeled datasets and domain-specific classifier adaptations. Their development of a web application for real-time damage classification also aligns with our objectives, though our scope is distinct, focusing on integrating aerial IR data with machine learning for near-real-time assessment.

Complementing this approach is the DamageMap classifier by Galanis et al. [2], which operates exclusively on post-wildfire aerial imagery to identify damaged buildings using a ResNet-based model architecture. DamageMap has shown robust generalizability with high accuracy across diverse test datasets, including data from the Camp and Carr wildfires. Their method, which does not require pre-disaster imagery, is particularly beneficial given the unpredictability of wildfires. This aligns with our approach, which can leverage both post-event and ongoing wildfire data. Similarly, ESRI provides a commodity tool with similar techniques [10]. Our approach has the added advantage of incorporating thermal infrared (IR) data from FIRIS to enhance visibility through smoke and other obstructions during real-time damage assessments.

Further advancing this field, Ahn et al. present DAVI (Disaster Assessment with Vision Foundation Model) [3], which introduces a novel approach for damage assessment across diverse geographic landscapes and disaster types. DAVI employs a foundation model in a change detection framework using before-and-after satellite images to overcome domain disparities and detect structural damage without requiring

ground-truth labels for the target region. Their model generates pseudo-labels based on a segmentation model (such as SAM [4]), followed by a two-stage refinement process that adjusts both pixel- and image-level accuracy. Evaluations across different terrains and disaster types (e.g., wildfires, hurricanes, earthquakes) demonstrate DAVI’s robustness in damage detection, reinforcing its suitability for rapid assessment in varied disaster scenarios. However, their reliance on pre- and post-disaster satellite RGB images, rather than aerial infrared imagery, limits DAVI’s applicability in certain scenarios, such as during active wildfires. The smoke cloud cover during such events obstructs satellite-based RGB imagery, making the approach unsuitable for near real-time damage assessment or response during ongoing fires. Together, these advancements underscore the expanding role of AI in improving the speed, accuracy, and scalability of damage assessment, setting the stage for further innovations in disaster response across various imaging modalities and environmental contexts.

The novel contributions of our paper include the use of aerial thermal infrared images captured by FIRIS aircraft, providing essential information absent in ground-based or satellite images. Ground-based image collection requires manual data gathering by specialized teams, which can only occur post-fire and is often impractical for covering large areas. Additionally, our data preprocessing method to align structures in aerial images with ground-truth damage points is based on an innovative buffer-based algorithm that optimally matches CAL FIRE damage points to building footprints without compromising accuracy. This approach ensures that our damage labels are accurately associated with the correct structures, making our predictive model and results highly reliable.

III. DATASET

When a wildfire starts, firefighting assets respond via ground and air to suppress the fire. The innovative FIRIS [11] program is specifically aimed towards providing real-time data from aircraft to crews on the ground using a wide range of sensors including multispectral cameras that capture aerial images of the fire spread. FIRIS [11] uses the Overwatch TK9 system, which consists of multiple frequency bands: visible spectrum (RGB), near-infrared (NIR), short-wavelength infrared (SWIR), medium-wavelength infrared (MWIR), and long-wavelength infrared (LWIR). In the early stages of a fire, smoke occludes visibility; therefore, the thermal infrared images are used to map the extent of the fire to capture images through smoke, as shown in Figure 1. In this work, specifically, we use MWIR images as they provide a good trade-off between successive image overlap and intensity contrast between fire and non-fire regions, which will allow a machine learning system to learn to distinguish between fire-damaged and non-damaged structures in a region. To process the aerial MWIR image sequences, we stitch the images together to create an image mosaic. We use photogrammetric software to simplify the process of mosaic creation and precise georectification.

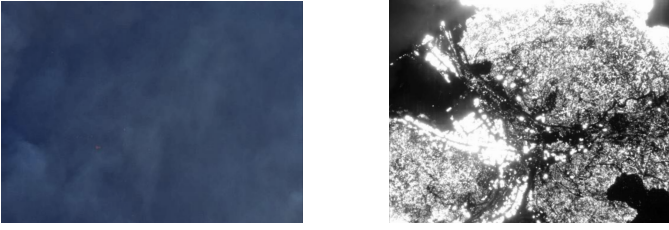


Fig. 1: Aerial photographs of downtown Greenville (CA) captured on August 5, 2021 contrasting the difference between Visible spectrum image (RGB) (left) and mid-wavelength infrared (MWIR) band (right) during a fire. RGB image is covered with smoke whereas MWIR image shows bright intensity in fire-affected regions and dark for unaffected regions.

IV. DATA PREPROCESSING

A. Mosaic Creation

Mosaics are generated by stitching together a sequence of images successively captured by the FIRIS TK9 sensor, covering partially overlapping regions. The imagery is recorded with metadata, including associated timestamps, image extent information, camera position, orientation, and more. To create accurate georeferenced mosaics from these partially overlapping images, we use a software tool called Agisoft Metashape Professional [7], which uses the image sequence and metadata to stitch them together into a single mosaic image. The process aligns the images, creates a dense point cloud and mesh of the captured region, and generates an orthomosaic. In our current workflow, the mosaic needs to be generated manually by a human to precisely identify ground control points, and the entire process takes approximately 10 minutes for a roughly 1,000-image sequence on a MacBook M1 computer. We follow a methodology similar to that presented in [8] for generating mosaics.

B. Data Association

After a wildfire has burned through a region, CAL FIRE inspection teams are dispatched to manually assess the damage by collecting damage inspection data (DINS) related to structures in the affected areas. These teams gather various types of information related to damaged or undamaged structures, including the type of structure, geographic coordinates, and extent of damage. In this work, we use DINS post-fire damage assessment as a labeled dataset [9]. DINS categorizes structural damage caused by wildfires into several levels based on severity: Destroyed (>50%), Major (26-50%), Minor (10-25%), Affected (1-9%), No Damage, and Inaccessible. The table in Figure 2 shows examples of post-fire damage assessments collected by the DINS team for various wildfires in recent years. These damage reports provide ground-truth labels that can be associated with aerial images collected during wildfires to train a machine learning model for structural damage prediction in near-real time. The first step in our data integration pipeline is to establish a

geometry	damage	fire_id	structuretype
POINT (-120.51163 38.64119)	Destroyed (>50%)	caldor2021	Single Family Residence Multi Story
POINT (-120.94183 40.13938)	No Damage	dixie2021	Commercial Building Single Story
POINT (-120.40454 38.77506)	No Damage	caldor2021	Single Family Residence Multi Story
POINT (-120.61381 38.62046)	No Damage	caldor2021	Utility Misc Structure
POINT (-119.88423 37.51760)	Destroyed (>50%)	oak_2022	Motor Home

Fig. 2: Examples of CAL FIRE post-fire damage assessments collected by human inspection teams

correspondence between the DINS points shown in Figure 2 and the mosaics created from the aerial images to capture the infrared signatures of damaged and undamaged structures within the fire-affected regions. This process associates structures labeled in the DINS data to the aerial imagery and allows for the determination of their bounding box geometries. The DINS data consists of point-based GPS locations (latitude, longitude) and human-labeled damage categories for structures in the region. However, since these geolocations are manually recorded, they do not precisely correspond to the exact location of the structures and may reflect GPS readings taken near, but outside, the structure perimeter. Additionally, the damage reports do not include shape or boundary information for the structures. To estimate their shape and size, and to address inaccuracies in the DINS geolocations, we utilize building footprint data collected from two sources: Microsoft [12] and FEMA (Federal Emergency Management Agency) [13]. Building footprints provide information about structures, including their latitude, longitude, bounding box geometry, area, and more.

Microsoft’s building footprints are generated using deep neural networks for semantic segmentation applied to satellite images, offering a recent and accurate representation of buildings in a given region. In contrast, FEMA’s building footprints are also derived using satellite-based images and somewhat older but still valuable for our analysis. These ML methods work well for open spaces, but can miss buildings in places with tree coverage. Due to ongoing development and destruction from natural disasters like wildfires, these footprint datasets may not fully match the actual structures present at the time of the wildfires. Additionally, discrepancies between the FEMA and Microsoft footprints exist, with some structures appearing in only one dataset or in both. Even when a building is included in both datasets, slight variations in geolocation and bounding box geometries are common, as shown in Figure 3.

To associate labeled damage points with their corresponding building locations and bounding box geometries, we developed a robust iterative buffer-based matching algorithm. As mentioned earlier, DINS points may be geolocated inside or in close proximity to the structures. In our approach, DINS points are matched to the nearest building footprint by expanding the boundaries of each footprint incrementally. Buffered footprints refer to the original building footprints with an expanded boundary, as shown in Figure 3. The process begins with a buffer size of 0 meters, where DINS

Fire	No Damage	Affected (1-9%)	Minor (10-25%)	Major (26-50%)	Destroyed (>50%)	Inaccessible
Caldor 2021	3356	56	18	7	1006	2
Dixie 2021	2255	66	13	11	1304	7
Oak 2022	427	6	2	2	194	0

TABLE I: Number of CAL FIRE Damage Inspection (DINS) points per damage label for different fires

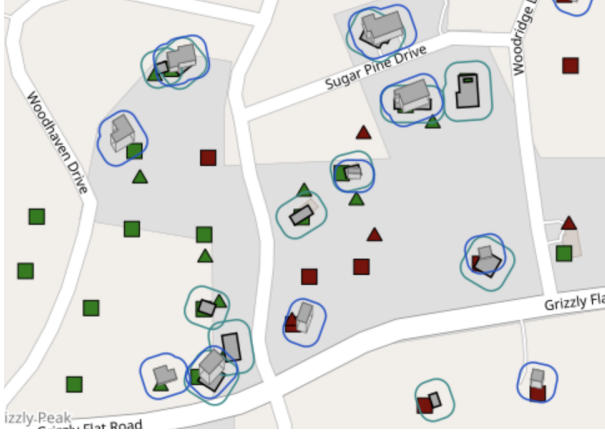


Fig. 3: Visualization of Microsoft and FEMA building footprints with a 10-meter buffer shown as blue and green bounding boxes, respectively. The 3D shapes represent Microsoft building footprints, while the 2D bounding boxes correspond to FEMA buildings. Red (damage) and green (no damage) points indicate the GPS locations of DINS points recorded by CAL FIRE teams, with point shapes denoting structure type.

points are checked against the original building footprints to determine if they fall within the boundaries. Matched DINS points and their corresponding footprints are removed from subsequent iterations. For unmatched points, the buffer size is increased sequentially to 5, 10, and 15 meters, repeating the matching process at each step. In cases where a DINS point matches multiple buffered footprints, it is assigned to the nearest footprint based on Euclidean distance, ensuring a one-to-one correspondence. Buffer sizes were chosen through heuristic evaluation, as larger buffers introduce a higher risk of mismatches between DINS points and incorrect building footprints. The matching process ultimately results in a one-to-one mapping of DINS points to their respective building footprints, linking the GPS locations and damage labels of the damage inspection points with the corresponding structure’s bounding box geometries. These bounding box geometries are later used to extract infrared signatures from the imagery and generate a set of features for a machine learning pipeline. Our algorithm is designed to maximize the number of correct associations between damage inspection points and building footprints while minimizing incorrect matches. Any points that cannot be matched to a nearby building footprint are set aside for future refinement of the matching algorithm. Table II summarizes the number of matched and unmatched damage assessment points across different wildfires. The mean success rate of our matching algorithm is roughly 63%.

Fire	Matched	Unmatched	Matching Success (%)
Dixie 2021	2253	1568	58.96
Caldor 2021	2530	1881	57.36
Oak 2022	443	166	72.74

TABLE II: Number of damage inspection points matched one-to-one with buildings and the number of unmatched points for each fire.

V. FEATURE GENERATION

Following data association, we categorize DINS points into two sets: those with one-to-one matches to building footprints and those that remain unmatched. For the matched set, we focus on the footprint bounding box region and extract the heat intensities of pixels in the mid-wave infrared (MWIR) signature from the image mosaic created from aerial images captured during the fire event. As illustrated in Figure 4, fire-damaged buildings typically exhibit high MWIR intensity, while undamaged structures show lower intensity. Using this principle, we extract features from each mosaic region corresponding to a matched footprint.

Our approach is based on the hypothesis that fire-damaged structures should display higher mean MWIR intensity compared to undamaged structures. To capture this information, we calculate the minimum, maximum, and mean intensities as features for each matched footprint. These features are used to train a machine learning model capable of distinguishing between damaged and undamaged buildings. It is worth noting that in the current iteration of our work, we do not extract features for unmatched DINS points. Instead, we aim to minimize the number of unmatched points through ongoing improvements in our data association techniques. To further refine our analysis, we extract additional features from aerial imagery mosaics by cropping regions that correspond to buffered building footprints. For each cropped region, we compute a range of feature statistics, including but not limited to minimum, maximum, and mean intensities. These comprehensive features serve as inputs to machine learning models trained to differentiate between various damage categories with greater accuracy.

The core of our approach involves constructing a robust training dataset that incorporates building features derived from heat intensities observed in aerial images during a wildfire event. These features are then paired with corresponding damage labels obtained from official DINS reports. This

combination of high-resolution spatial data and authoritative damage assessments enables our models to learn complex patterns and relationships, potentially improving the accuracy and reliability of wildfire damage predictions.

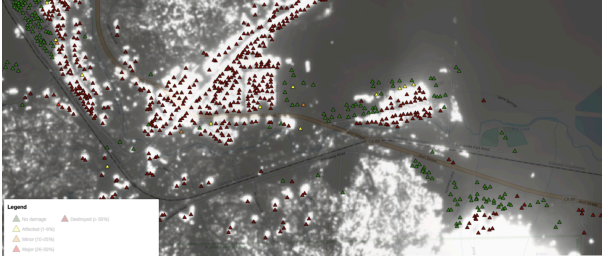


Fig. 4: Map of the Caldor Fire area in 2021 with an overlaid mosaic. Red points indicate structures labeled by DINS as damaged, while green points represent undamaged structures.

VI. MODEL IMPLEMENTATION

We implemented several machine learning classifiers to predict damage labels from the features generated as described previously. Our approach includes both simple models, such as logistic regression, and more complex ensemble-based methods, like decision trees and random forests, to assess the complexity of learning decision boundaries in the dataset. To ensure balanced representation of the different classes, we used an 80-20 (%) train-test split with stratified sampling, maintaining similar proportions of each class in both the training and testing sets. For the current iteration of this work, we excluded DINS points labeled as “Inaccessible” and consolidated certain damage categories. Specifically, we re-labeled points categorized as “Major (26-50%)”, “Minor (10-25%)”, and “Affected (1-9%)” as “Destroyed (>50%)” in order to emphasize binary classification - damaged versus non-damaged structures. This decision was made since the number of points in these intermediate categories is relatively small compared to the “Destroyed (>50%)” and “No Damage” categories, as shown in Table I. In future iterations, we plan to explore whether retaining the original multiclass labels improves classification performance, contributes to our goal of accurate damage assessment, and better supports response teams in their planning efforts.

For each random seed, hyperparameters were optimized using a 5-fold stratified cross-validated grid search on the training data. The optimal hyperparameters were then used to train a model on the entire training set. This process was repeated 10 times with different random splits to ensure robustness. Table III presents the mean classification accuracy and F1-scores achieved by various machine learning methods. Among these, the random forest classifier demonstrated superior overall performance on the held-out test sets, achieving a mean classification accuracy of 81.71% ($\pm 1.13\%$) and a mean F1-score of 84.35% ($\pm 1.06\%$).

Once the damage prediction model is trained and deployed, it can evaluate wildfire damage in near-real time, providing both a damage assessment and a confidence score for each assessment that reflects the model’s certainty. The inference process starts with the collection of aerial images captured during the early stages of a wildfire. These images are then processed to create mosaics, either manually by experts using software like MetaShape Pro [7] or through semi-automated tools, streamlining the data preparation for damage analysis. The mosaic creation process typically takes approximately 10 minutes per flight sequence. After the mosaics are generated, we extract mid-wave infrared (MWIR) signatures from these mosaics for each building footprint within the fire-affected area. These extracted features are then fed into the trained damage prediction model to infer the level of damage. The damage inference process, once the mosaic is generated, takes just a few seconds, leveraging distributed computing and parallel processing on a multi-core CPU. This efficient workflow ensures that our ML-based damage assessment system operates in near-real time, providing timely and actionable insights for effective wildfire management.

VII. CONCLUSION

Our objective in this work is to integrate multimodal data from aerial thermal imagery, post-fire manual damage assessment from CAL FIRE, and building footprints from satellite sources to develop a robust ML-driven system capable of accurately predicting wildfire-induced structural damage using only aerial imagery in near real-time during inference. By associating building footprints with damage labels and extracting features from thermal mosaics, we generated features and demonstrated the effectiveness of machine learning models in predicting structural damage. Our approach was validated across several representative wildfire events in California, showcasing its reliability, applicability, and scalability to real-world scenarios.

In this study, we demonstrated promising results using data from the Caldor 2021, Dixie 2021, and Oak 2022 wildfires. The results underscore the potential of integrating machine learning with aerial imagery to support effective disaster response by providing needed damage assessments. Our system offers a scalable solution that can provide emergency managers with timely and reliable damage assessments within the first operational period, typically within 24-48 hours of the start of a fire. This capability could significantly improve resource allocation, recovery planning, and overall emergency response.

VIII. FUTURE WORK

For future work, we aim to expand our dataset to include many more wildfires to enhance the generalizability of our model and to evaluate our model’s performance across a variety of environments. To improve data quality, we plan to create a more accurate building footprint dataset leveraging USGS 3DEP LiDAR data [14] to extract footprints and cross-referencing it with existing Microsoft [12] and FEMA

	Accuracy (%)				F1-Score (%)			
	Logistic Regression	SVM	Decision Tree	Random Forest	Logistic Regression	SVM	Decision Tree	Random Forest
Caldor 2021	67.44 \pm 2.33	77.67 \pm 1.4	77.67 \pm 1.02	78.5 \pm 0.87	71.02 \pm 2.11	83.46 \pm 0.98	83.54 \pm 0.79	83.73 \pm 0.64
Dixie 2021	89.92 \pm 1.76	82.35 \pm 0.99	90.5 \pm 1.11	91.18 \pm 1.97	90.69 \pm 1.76	85.87 \pm 0.85	91.33 \pm 1.08	91.97 \pm 1.86
Oak 2022	69.03 \pm 0.38	72.31 \pm 1.27	81.53 \pm 1.86	83.92 \pm 0.72	74.7 \pm 1.45	73.75 \pm 0.5	81.96 \pm 0.93	82.29 \pm 1.15
Combined	75.36 \pm 0.91	76.67 \pm 0.29	78.61 \pm 1.62	81.71 \pm 1.13	75.63 \pm 1.1	81.22 \pm 0.28	82.57 \pm 0.78	84.35 \pm 1.06

TABLE III: Mean accuracy and F1 scores (with standard deviation) across 10 runs with varying random seeds for different models, evaluated on individual wildfire data as well as combined data.

[13] footprint datasets. This will allow us to capture currently missing structures (such as regions with heavy tree coverage), increasing the number of matched labels and expanding our training dataset. Currently, we manually design features from multimodal data based on the assumption that damaged structures exhibit higher heat intensity, while non-damaged structures have lower intensity. We plan to automate feature generation within the ML pipeline by leveraging advanced deep neural networks such as convolutional neural networks (CNNs) (e.g., ResNet, U-Net) and Vision Foundation Models such as CLIP (Contrastive Language-Image Pretraining) [5], Segment Anything Model (SAM) [4], Detection Transformer (DETR) [6], etc. that can extract relevant features directly from mosaics, enabling end-to-end training and improving model generalization.

We aim to enhance our damage assessment model by incorporating multispectral imaging, combining RGB and infrared modalities. While infrared imaging is effective for distinguishing between damaged and intact structures during active fires due to thermal contrast, its utility diminishes in post-fire assessments once structures have cooled. In these post-fire conditions, high-resolution aerial RGB images offer a more reliable means of differentiating damaged from undamaged buildings, particularly when smoke is no longer a visual barrier. This multispectral approach promises to improve classification accuracy in various stages of fire, enabling more comprehensive and adaptable damage assessment capabilities.

We also aim to automate or eliminate the need for mosaic creation by exploring image-based approaches that can directly extract features from raw aerial images. This shift could enable real-time damage assessment, removing manual intervention, and enhancing both model accuracy and system usability. Additionally, we will explore extending our approach to other natural hazards, such as earthquakes and floods, broadening the methodology and expanding the system’s capability to assess a wider range of disaster scenarios. This will further enhance the versatility and utility of our AI-based damage assessment framework.

ACKNOWLEDGMENT

The authors would like to thank the WIFIRE Lab and WordS Center teams at the San Diego Supercomputer Center

for their support of this study. The authors also express their gratitude to Daniel Roten for his valuable contributions to this project. This work was funded in part by the California Governor’s Office of Emergency Services FIRIS program and National Science Foundation (NSF) Award 2134904 and NDP Grant 2333609.

REFERENCES

- [1] Luo, K.; Lian, I.-b. “Building a Vision Transformer-Based Damage Severity Classifier with Ground-Level Imagery of Homes Affected by California Wildfires,” *Fire*, vol. 7, no. 4, pp. 133, 2024. Available: <https://doi.org/10.3390/fire7040133>
- [2] Galanis, M.; Rao, K.; Yao, X.; Tsai, Y.-L.; Ventura, J.; Fricker, G.A. “DamageMap: A Post-Wildfire Damaged Buildings Classifier,” *International Journal of Disaster Risk Reduction*, vol. 65, 102540, 2021. Available: <https://doi.org/10.1016/j.ijdr.2021.102540>
- [3] Ahn, E.; Xu, Z.; Doermann, D.; Zhang, Z. “Generalizable Disaster Damage Assessment via Change Detection with Vision Foundation Model,” *arXiv preprint arXiv:2406.08020*, 2024. Available: <https://arxiv.org/abs/2406.08020>
- [4] Kirillov, A.; Mintun, E.; Ravi, N.; Mao, H.; Rolland, C.; Gustafson, L.; Xiao, T.; Whitehead, S.; Berg, A.C.; Lo, W.-Y.; Dollár, P.; Girshick, R. “Segment Anything,” *arXiv preprint arXiv:2304.02643*, 2023. Available: <https://arxiv.org/abs/2304.02643>
- [5] Radford, A.; Kim, J.W.; Hallacy, C.; Ramesh, A.; Goh, G.; Agarwal, S.; Sastry, S.; Askell, A.; Mishkin, P.; Clark, J.; Krueger, G.; Sutskever, I. “Learning Transferable Visual Models from Natural Language Supervision,” *Proceedings of the 38th International Conference on Machine Learning*, vol. 139, pp. 8748–8763, 2021. Available: <https://arxiv.org/abs/2103.00020>
- [6] Carion, N.; Massa, F.; Synnaeve, G.; Usunier, N.; Kirillov, A.; Zagoruyko, S. “End-to-End Object Detection with Transformers,” *Proceedings of the European Conference on Computer Vision (ECCV)*, vol. 12346, pp. 213–229, 2020. Available: <https://arxiv.org/abs/2005.12872>
- [7] Agisoft Metashape Professional (Version 2.0.3) (Software). (2024). Available: <https://www.agisoft.com/downloads/installer/>
- [8] “Agisoft Metashape Image Processing Digital Aerial Imagery,” GTAC, U.S. Forest Service, 2021. Available: fsapps.nwccg.gov
- [9] CAL FIRE Post-Fire Damage Assessment Dataset. Available: fire.ca.gov
- [10] Schultz, A.; Perez, J. “GIS and Deep Learning Make Damage Assessments More Timely and Precise,” *Journal ArcUser*, 2024. Available: <https://www.esri.com/about/newsroom/wp-content/uploads/2024/01/lahaina.pdf>
- [11] Cal OES Fire Integrated Real-time Intelligence System. Available: <https://wifire.ucsd.edu/firis-in-depth>
- [12] Microsoft Global Building Footprints. Available: <https://github.com/microsoft/GlobalMLBuildingFootprints>
- [13] FEMA Building Footprints Dataset. Available: <https://gis-fema.hub.arcgis.com/pages/usa-structures>
- [14] USGS 3DEP LiDAR Dataset. Available: <https://www.usgs.gov/3d-elevation-program/what-3dep>
- [15] California Governor’s Office of Emergency Services. Available: caloes.ca.gov